

## Polarisation-sensitive terahertz detection by multicontact photoconductive receivers

E. Castro-Camus,\* J. Lloyd-Hughes, and M.B. Johnston  
*University of Oxford, Department of Physics, Clarendon Laboratory,  
 Parks Road, Oxford OX1 3PU, United Kingdom*

M.D. Fraser, H.H. Tan, and C. Jagadish  
*Department of Electronic Materials Engineering, Research School of Physical Sciences and Engineering,  
 Institute of Advanced Studies, Australian National University, Canberra ACT 0200, Australia*  
 (Received 10 March 2005; Accepted 18 May 2005)

We have developed a terahertz radiation detector that measures both the amplitude and polarisation of the electric field as a function of time. The device is a three-contact photoconductive receiver designed so that two orthogonal electric field components of an arbitrary polarised electromagnetic wave may be detected simultaneously. The detector was fabricated on  $\text{Fe}^+$  ion-implanted InP. Polarisation-sensitive detection is demonstrated with an extinction ratio better than 100:1. This type of device will have immediate application in studies of birefringent and optically active materials in the far-infrared region of the spectrum.

PACS numbers: 07.50.-e, 07.57.-c, 07.57.Kp, 07.57.Pt, 07.60.Fs, 42.25.Ja, 71.55.Eq, 78.20.Ek, 78.20.Fm

The far-infrared, or terahertz (THz), region of the electromagnetic spectrum encompasses the energy range of many collective processes in condensed matter physics and macromolecular chemistry. However, in the past this spectral region has been relatively unexplored owing to a lack of bright radiation sources and appropriate detectors. The technique of THz time domain spectroscopy (TDS),<sup>1,2</sup> which has developed rapidly as a result of advances in ultra-short pulsed laser technology, now provides a very sensitive probe across the THz band. TDS is currently an invaluable tool in condensed matter physics<sup>3,4,5</sup> and macromolecular chemistry.<sup>6,7</sup>

To date THz-TDS techniques have relied on linearly polarised emitters and detectors. However, for spectroscopy of birefringent and optically active materials it is also important to measure the polarisation state of radiation before and after it has interacted with the material. Here we report on a detector that enables such a THz-TDS system to be realised.

Vibrational circular dichroism (VCD) spectroscopy is a new technique which has substantial potential in the fields of macromolecular chemistry and structural biology.<sup>8</sup> Akin to the established technique of (ultraviolet) circular dichroism, VCD is used to analyse the structure of chiral molecules. It is predicted that VCD will be more powerful than conventional circular dichroism for stereo-chemical structure determination.<sup>8</sup> However the technique is currently limited by insensitive and narrow band spectrometers.

Of particular interest to biochemists is the structure and function of proteins and nucleic acids. These chiral biomolecules have vibrational and librational modes in the THz region and the THz optical activity of these modes are starting to be studied experimentally.<sup>9,10</sup> THz frequency VCD is already finding application in fields as distinct as biochemical research<sup>11</sup> and astrobiology.<sup>10</sup> In

the future the ability to perform VCD using a polarisation sensitive THz-TDS technique should enhance the bandwidth and sensitivity of measurements, and allow dynamic time-resolved studies to be performed.

In order to perform polarisation sensitive THz-TDS, it is necessary to be able to measure two (preferably orthogonal) electric field components of a terahertz transient. Theoretically it is possible to do this using a conventional (two contact) photoconductive receiver. That is, measure one electric field component and then rotate the receiver by  $90^\circ$  and measure the other component. However in practice this procedure has two major disadvantages: Firstly, during the rotation of the photoconductive receiver, any slight misalignment will significantly shift the relative phase of the electric field components; secondly the data acquisition time is increased as both components are recorded separately. In order to avoid these disadvantages an integrated receiver capable of measuring both components simultaneously is needed. Such a detector may be realised by fabricating a three-contact photoconductive receiver.

The three-contact receiver we developed is shown in Fig. 1. When designing the three-contact receiver we considered two main constraints. Firstly, the unit vectors ( $\hat{\mathbf{u}}_1$  and  $\hat{\mathbf{u}}_2$ ) normal to the gaps formed between the earth contact and the other two contacts (1 and 2) need to be orthogonal. Secondly it is necessary that both gaps are within an area smaller than the laser beam waist and the focus spot size of the THz radiation (a circle of radius  $\sim 100 \mu\text{m}$ ). This last condition is necessary in order to have uniform laser and THz illumination across both gap regions.

The performance of a photoconductive receiver depends strongly on the material from which the device is fabricated. Material dependent carrier trapping and recombination times play an essential role in photoconduc-

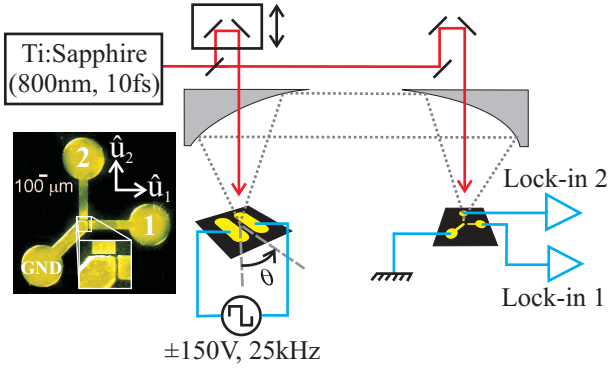


FIG. 1: (Colour online) Diagram of experimental apparatus used for simultaneous detection of horizontal and vertical components of the electric field of a THz transient. A SI-GaAs photoconductive switch was used as emitter, parabolic mirrors were used to collect and focus the THz radiation onto the three-contact photoconductive receiver. One of the contacts was used as common (GND) and the other two were amplified independently to obtain the two orthogonal components. Inset: Photograph of a three-contact photoconductive receiver structure formed by two  $16\mu\text{m}$  gaps in orthogonal directions in order to measure the perpendicular components of the THz electric field. The unit vectors  $\hat{\mathbf{u}}_1$  and  $\hat{\mathbf{u}}_2$  represent the directions between the earth contact and contacts 1 and 2 respectively. The photograph was taken using an optical microscope.

tive receiver device performance. Specifically, long carrier lifetimes will permit the reception of large amounts of noise and short carrier lifetimes will reduce the signal level and accuracy. Modified semiconductor materials such as low-temperature-grown or ion-implanted GaAs/InP are typically used, as carrier trapping times in these materials may be controlled.<sup>12,13</sup>

In order to fabricate the three-contact PCS device (shown in Fig. 1) we have implanted semi-insulating InP (100) substrates using 2.0 MeV and 0.8 MeV  $\text{Fe}^+$  ions with doses of  $1.0 \times 10^{13} \text{ cm}^{-2}$  and  $2.5 \times 10^{12} \text{ cm}^{-2}$  respectively. These multi-energy implants gave an approximately uniform density of vacancies to a depth of  $1\mu\text{m}$ , resulting in a carrier lifetime of  $\sim 130 \text{ fs}$ .<sup>14</sup> The samples were subsequently annealed at  $500^\circ\text{C}$  for 30 minutes under a  $\text{PH}_3$  atmosphere. Finally the electrodes were defined using standard photolithography and lift-off techniques. The Cr/Au contacts were deposited to a thickness of 20/250 nm using a thermal evaporator.

In order to measure a THz electric field  $\mathbf{E}_{\text{THz}}$  using a photoconductive receiver it is necessary to gate the receiver with an ultra-short laser pulse. The laser pulse generates free charge carriers in the semiconductor substrate, which are accelerated by  $\mathbf{E}_{\text{THz}}$  thus generating a current  $I$  between two contacts. Assuming a laser pulse of the form  $\text{sech}^2(1.76t/t_0)$  where  $t_0$  is the full-width-at-half-maximum, the current measured through contact  $i$  in the photoconductive receiver described here, is related to  $\mathbf{E}_{\text{THz}}$  by<sup>15</sup>:

$$I_i(t) \propto \int_{-\infty}^{\infty} \mathbf{E}_{\text{THz}}(t') \cdot \hat{\mathbf{u}}_i e^{-(t'-t)/\tau} \times [1 + \tanh(1.76(t' - t)/t_0)] dt' \quad (1)$$

where  $\mathbf{E}_{\text{THz}}(t')$  is the THz electric field,  $\hat{\mathbf{u}}_1$  and  $\hat{\mathbf{u}}_2$  are unit vectors in the direction of the two gaps between the contact ( $i = 1, 2$ ) and the earth electrode.  $\tau$  is the lifetime of free carriers.

The three-contact photoconductive receiver was tested using the setup shown in Fig. 1. A linearly polarised THz transient was generated by exciting a  $400\mu\text{m}$  gap SI-GaAs photoconductive switch emitter biased by a  $\pm 150 \text{ V}$  square wave at a frequency of  $25 \text{ kHz}$ . The emitted THz transients were collected in the back reflection geometry and then focused on to the receiver using off-axis parabolic mirrors. A Ti:Sapphire chirped mirror oscillator with a  $75 \text{ MHz}$  repetition rate provided  $10 \text{ fs}$  pulses of  $4 \text{ nJ}$  and  $800 \text{ nm}$  centre wavelength, which were used to excite the emitter. A  $0.4 \text{ nJ}$  fraction split from the original pulse was used to gate the receiver.

Two separate lock-in amplifiers were used to record the currents ( $I_1$  and  $I_2$ ) through the two contacts. The lock-in amplifiers and the common electrode of the receiver were connected to a common earth, and the references

of both lock-in amplifiers were locked to a TTL signal provided by the  $25 \text{ kHz}$  signal generator (used to drive the THz emitter). In all measurements the  $I_1(t)$  signal from Lock-in 1 and  $I_2(t)$  signal from Lock-in 2 were recorded simultaneously at each time step using a multichannel analogue to digital converter.

The photoconductive switch emitter was mounted on a graduated rotation stage that allowed the gap, and hence the polarisation of the emitted THz transient, to be rotated. Both  $I_1(t)$  and  $I_2(t)$  were measured averaging over 90 scans at three different angles of the emitter ( $0^\circ$ ,  $45^\circ$  and  $90^\circ$ ). The measurements were taken in an evacuated chamber at a pressure of  $25 \text{ mbar}$  to avoid water vapor absorption. The THz electric field was calculated by differentiating numerically the two  $I(t)$  traces measured by the lock-in amplifiers according to Eq. 1. The horizontal  $E_H$  and vertical  $E_V$  electric field components are plotted against time in Figs. 2 (a), (b) and (c) for the emitter at angles  $0^\circ$ ,  $45^\circ$  and  $90^\circ$  respectively. The results demonstrate that the three-contact photoconduc-

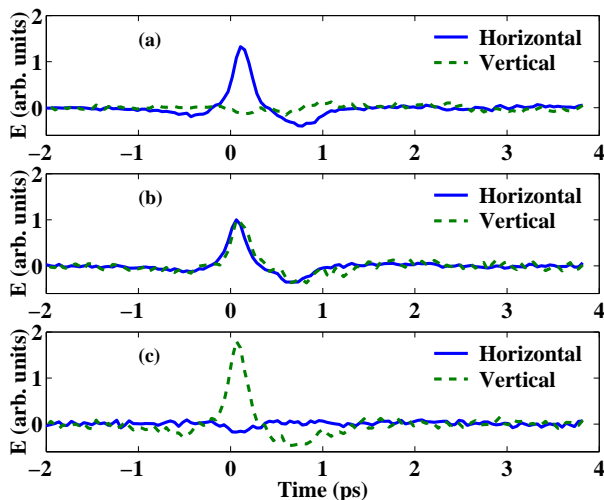


FIG. 2: (Colour online) Horizontal (solid) and vertical (dashed) components of THz electric field (obtained from measured voltage) are plotted against time with the emitter at (a) 0, (b) 45 and (c) 90° respectively.

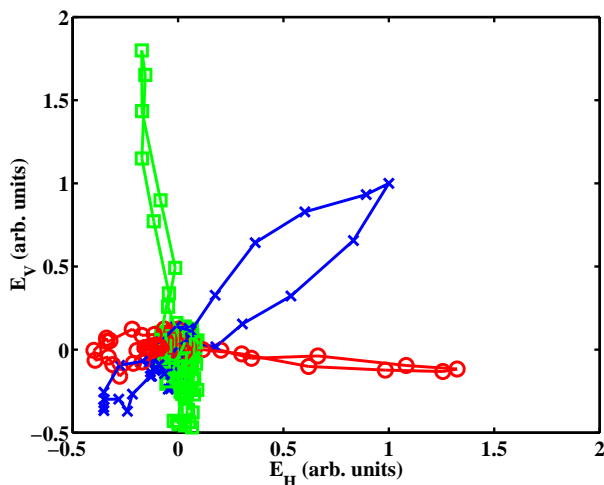


FIG. 3: (Colour online) Parametric representation of horizontal and vertical components of THz electric field for three emitter orientations; 0 (circles), 45 (crosses) and 90° (squares). The THz wavevector points out of the paper plane. In this plot the angle of polarisation for the three waves is easily observed.

tive receiver acts as a polarisation sensitive detector. The

polarisation selectivity of the detector was assessed by measuring the cross polarised extinction ratio. This ratio was found to be 108:1 (128:1) for the horizontally (vertically) oriented emitter. It should be noted that the polarisation of the radiation arriving at the detector may not be perfectly linear, as photoconductive emitters do not produce purely dipolar radiation.<sup>16</sup> Therefore, the true extinction ratio of the detector may be higher.

In Fig. 3 a parametric plot of the data shown in Fig. 2 is presented. For an ideal linearly polarised source the three sets of data should form straight lines at 0, 45 and 90° in the  $E_H - E_V$  plane. However, the measured angles of polarisation (from the horizontal plane) are -5.5, 39, and 98° respectively and the polarisation appears to be slightly elliptical (especially in the 45° case). These discrepancies arise from a number of sources: It has been shown previously that photoconductive switch emitters produce a small quadrupole field leading to a cross polarised electric field component.<sup>16,17</sup> Furthermore, low  $f$ -number collection systems (such as the  $f/1.5$  system used in this experiment) inevitably lead to linearly polarised radiation becoming slightly elliptical.<sup>16</sup>

The signal-to-noise (SNR) ratio in our experiments was measured to be 175:1 for the three contact receiver. We obtained a similar ratio for a conventional two-contact “bow-tie” receiver, which we fabricated on a piece of the same substrate material. This indicates that the SNR performance of this device is limited by the substrate material rather than the receiver design. Therefore the device sensitivity could be improved greatly by using optimised ion-implanted InP or GaAs substrates. Indeed optimised low temperature MBE-grown GaAs has been shown to have excellent SNR performance<sup>13</sup> which should be replicated in a three-contact device fabricated on that material.

In conclusion, the design of a novel integrated detector capable of measuring both components of an arbitrarily polarised THz transient was presented as well as experimental evidence of its effectiveness. This integrated three-contact detector is expected to be very useful for further studies of time-domain circular dichroism spectroscopy and should have a wide range of applications in basic research and industry.

The authors would like to thank the EPSRC (UK) and the Royal Society for financial support of this work, ECC wishes to thank CONACyT (México) for a scholarship. Australian authors would like to acknowledge the financial support of the Australian Research Council.

\* Electronic address: e.castro-camus1@physics.ox.ac.uk

<sup>1</sup> D. H. Auston and K. P. Cheung, J. Opt. Soc. Am. B **2**, 606 (1985).

<sup>2</sup> P. R. Smith, D. H. Auston, and M. C. Nuss, IEEE J. Quantum Electron. **24**, 255 (1988).

<sup>3</sup> R. Huber, F. Tauser, A. Brodschelm, M. Bichler, G. Abstreiter, and A. Leitenstorfer, Nature **414**, 286 (2001).

<sup>4</sup> A. Leitenstorfer, R. Huber, F. Tauser, A. Brodschelm, M. Bichler, and G. Abstreiter, Physica B **314**, 248 (2002).

<sup>5</sup> R. A. Kaundl, D. Hagele, M. A. Carnahan, R. Lovenich,

- and D. S. Chemla, *Phys. Status Solidi B* **238**, 451 (2003).
- <sup>6</sup> M. Johnston, L. Herz, A. Khan, A. Köhler, A. Davies, and E. Linfield, *Chem. Phys. Lett.* **377**, 256 (2003).
  - <sup>7</sup> C. A. Schmuttenmaer, *Chem. Rev.* **104**, 1759 (2004).
  - <sup>8</sup> L. A. Nafie, *Applied Spectroscopy* **50**, 12A (1996).
  - <sup>9</sup> J. Xu, J. Galan, G. Ramian, P. Savvidis, A. Scopatz, R. R. Birge, S. J. Allen, and K. Plaxco (SPIE, 2004), vol. 5268, pp. 19–26.
  - <sup>10</sup> J. Xu, G. Ramian, J. Galan, P. Savvidis, A. Scopatz, R. Birge, J. Allen, and K. Plaxco, *Astrobiology* **3**, 489 (2003).
  - <sup>11</sup> W. R. Salzman, *J. Chem. Phys.* **107**, 2175 (1997).
  - <sup>12</sup> T.-A. Liu, M. Tani, M. Nakajima, M. Hangyo, K. Sakai, S. ichi Nakashima, and C.-L. Pan, *Optics Express* **12**, 2954 (2004).
  - <sup>13</sup> Y. C. Shen, P. C. Upadhyaya, H. E. Beere, E. H. Linfield, A. G. Davies, I. S. Gregory, C. Baker, W. R. Tribe, and M. J. Evans, *Appl. Phys. Lett.* **85**, 164 (2004).
  - <sup>14</sup> C. Carmody, H. H. Tan, C. Jagadish, A. Gaarder, and S. Marcinkevicius, *J. Appl. Phys.* **94**, 1074 (2003).
  - <sup>15</sup> S. Kono, M. Tani, and K. Sakai, *Appl. Phys. Lett.* **79**, 898 (2001).
  - <sup>16</sup> J. V. Rudd, J. L. Johnson, and D. M. Mittleman, *J. Opt. Soc. Am. B* **18**, 1524 (2001).
  - <sup>17</sup> Y. Cai, I. Brener, J. Lopata, J. Wynn, L. Pfeiffer, and J. Federici, *Appl. Phys. Lett.* **71**, 2076 (1997).